Fuel Processing Technology 129 (2015) 39–51

Contents lists available at ScienceDirect

Fuel Processing Technology

journal homepage: www.elsevier.com/locate/fuproc

Co-combustion of brewer's spent grains and Illinois No. 6 coal: Impact of blend ratio on pyrolysis and oxidation behavior

Ana M. Celaya [a], Amanda T. Lade [a], Jillian L. Goldfarb [b,*]

[a] Department of Chemical Engineering, University of New Hampshire, 33 Academic Way, Durham, NH 03824, United States
[b] Department of Mechanical Engineering and Division of Materials Science & Engineering, Boston University, 110 Cummington Mall, Boston, MA 02215, United States

ARTICLE INFO

Article history:
Received 10 October 2013
Received in revised form 31 July 2014
Accepted 2 August 2014
Available online xxxx

Keywords:
Biomass
Coal
Co-combustion
Pyrolysis
Oxidation
Activation energy

ABSTRACT

Co-combustion of locally available biomass in existing coal-fired power plants is an attractive option to increase the share of renewable fuels in the energy market with minimal capital investment. Utilizing existing coal-fired combustion equipment for blends requires knowledge of pyrolysis and combustion characteristics. This study presents thermal evolution profiles (decomposition rates, apparent activation energies and devolatilized compounds) of coal–biomass blends to probe the effect of blend ratios on pyrolysis and combustion behavior. The global rate of pyrolysis of Illinois No. 6 coal and brewer's spent grains (BSG) is a function of fuel composition, though analysis of evolved gases suggests the presence of both potential additive and synergistic interactions on a molecular level. For oxidation, a rapid decrease in peak conversion rate is seen as the percentage of BSG increases from 0% to 20%, becoming less pronounced as the percentage of BSG increases above 20%.

1. Introduction

Almost half of the electricity in the United States is generated by burning coal, a process that emits vast amounts of carbon dioxide and produces a flue gas laden with sulfur and nitrogen oxides [1]. The environmental impacts of the mining, transport, and combustion of coal, along with questions surrounding its future supply levels, have led to considerable research on alternative and renewable fuels, including biomass. Second-generation biomass feedstocks, comprised of agricultural wastes and organic byproducts, may provide a bridge between conventional fossil fuel sources and a renewable energy future. Given that much of today's electricity infrastructure is devoted to coal combustion, a likely avenue in the near future for biomass utilization is as a blended feedstock with coal.

While the low sulfur content of most biomass has the potential to reduce overall SO_x emissions, as well as net CO_2 emissions from a coal-fired power plant [1,2], the higher proportion of oxygen and hydrogen to carbon atoms in biomass does result in a lower heating value for biomass than coal [3]. However, the higher oxygen content of biomass also tends to give it a higher reactivity than coal, and thus a lower activation energy barrier to devolatilization and oxidation [4,5]. Ash deposition from the combustion of pure biomass streams results in fouling and slagging on heat exchanger surfaces in the boilers [6]. To overcome the issues associated with pure biomass combustion, existing pulverized coal-fired boilers across the world blend biomass in varying proportions with coal. Optimizing operating conditions for such fuel blending requires a greater understanding of the thermal characteristics and combustion kinetics of coal–biomass blends [7,8]. Currently, much of the research on coal–biomass blends originates from Europe and Asia on coals of regional origin with varying volatile and chemical compositions, blended with biomass specific to those regions, such as palm oil in Malaysia [9] and olive kernels in Greece [10]. In the Northeast region of the United States, readily available biomass includes forest and agricultural byproducts and industrial organic waste, including spent barley and hops from local breweries. Brewer's spent grain (BSG) is 85 wt.% of the total by-product generated in the brewing process and is produced year-round by breweries across the country [11].

Our focus on a locally available biomass source such as BSG is intended to mitigate the long-range transport of fuels (thereby decreasing both the cost and carbon footprint of the fuel). There are 16 commercial breweries in the state of New Hampshire alone, three of which are located in Portsmouth, near Schiller Station, a 150 MW station with two 50 MW coal-fired boilers. While BSG exits the brewing process as a wet stream, in many cases the wastewater produced may not be discarded. Breweries, such as Redhook Ale Brewery in Portsmouth and Anheuser-Busch Brewery in Merrimack, NH, use microbes to treat the water, producing methane. This methane could be used as a heat source to dry the solid BSG on-site for transport to a local coal-fired power plant.

Like coal, biomass is a carbonaceous fuel that will undergo a series of steps from pyrolysis to oxidation. Pyrolysis—the thermal decomposition

* Corresponding author. Tel.: +1 617 353 3883.
E-mail addresses: JillianLGoldfarb@gmail.com, jilliang@bu.edu (J.L. Goldfarb).

http://dx.doi.org/10.1016/j.fuproc.2014.08.004
0378-3820/

of a solid in the absence of oxygen—is rapidly gaining attention itself as a thermochemical conversion process to obtain fuels from biomass [12–15]. Pyrolysis is also the first step in thermochemical conversion via oxidation [10]. The volatiles released during pyrolysis undergo oxidation within the gas layer surrounding the particles. The char remaining after the pyrolysis and ensuing volatile combustion is essentially fixed carbon; when the volatiles are exhausted, oxygen will diffuse towards the char surface and combustion ensues. Because the composition of biomass varies from source to source, a blanket reactivity profile for the pyrolysis and oxidation of a specific lignocellulosic biomass material is not applicable across all biomass types. On a dry basis, barley straw contains approximately 20% hemicellulose, 33% cellulose, 17% lignin, 2.2% ash, and the remainder of proteins and fat [16]. For comparison, wood contains 39–41% cellulose, 24–35% hemicellulose, and 20–28% lignin on a dry basis [17].

Although each type of biomass exhibits different thermal decomposition profiles, the pyrolysis of biomass generally yields global activation energies within similar ranges. When analyzed using the Arrehnius method under a first order global reaction scheme, most biomasses show three distinct devolatilization regions (suggesting three distinct activation energies) with abrupt transitions, roughly corresponding to the hemicellulose, cellulose and lignin fractions of the biomass. The pyrolysis of hemicellulose occurs approximately between 220 and 315 °C, cellulose from 315 to 400 °C, and lignin over a range of 160–900 °C [18]. Grammelis et al. [19] find activation energies of the pyrolytic decomposition of the primary components (hemicellulose, cellulose, lignin) of waste paper biomass of 107–164, 198–232, and 30–48 kJ/mol, respectively, at a heating rate of 20 °C/min under the assumption of multiple degradation reactions occurring simultaneously with a summative reaction order of one. Also under a first order reaction scheme, our laboratory found activation energies of pyrolysis of cabbage palm biomass with ranges of 64–115, 67–152 and 19–25 kJ/mol for the same three fractions under heating rates ranging from 25 to 100 °C/min [20]. Interestingly, activation energies for the pyrolysis of coal–biomass blends fall into a similar range as those of pure biomass, with the activation energies increasing as the amount of coal increases, such as those noted by Vuthaluru [3] in the pyrolysis of a Collie subbituminous coal and wheat straw.

Under oxidative conditions, many analyses using the Arrenhius method find two decomposition regimes, corresponding to a lumped pyrolysis/oxidation of volatiles, and a second step for char oxidation. Gil et al. [5] studied the co-combustion of high-volatile bituminous coal blended with pine sawdust, suggesting that biomass combustion takes place in two steps over a low temperature range (200–490 °C), while coal combusted in a single step (315–615 °C); they found the co-combustion of these solid fuels to be additive, as three steps occurred during the process. Like pyrolysis, the activation energies of oxidation increased with increasing coal content in initial stages of degradation, however, Gil et al. did find that for a greater than 80 wt.% coal content, the kinetic parameters increase dramatically—more so than perhaps an additive scheme would suggest.

There is a question of synergistic (non-additive) effects occurring with blended fuel pyrolysis and oxidation reactions. Some groups find that the kinetics of pyrolysis and oxidation of blended biomass and coal are somewhat additive in nature, whereby each fuel contributes to the activation energy and peak devolatilization rates proportionally to the blend ratios [5,9,21,22]. Other studies suggest synergistic reaction chemistry during biomass–coal co-firing, lowering overall activation energies for the combustion of blends as compared to an additive scheme of coal plus biomass activation energies [23–25]. While biomass exhibits lower heating values than coal, it tends to release volatiles more rapidly during the pyrolysis stage of combustion, [23] and as such the overall decomposition profiles are necessary to determine the optimal blend ratio(s) for a given biomass and coal in co-combustion.

2. Materials and methods

2.1. Materials

One local source of biomass in Southeastern New Hampshire is the spent barley and hops from the many commercial breweries. To measure the reaction kinetics of this biomass and coal, brewer's spent grains (BSG) were collected from Redhook Brewery immediately following the malting process, dried in an oven at 105 °C overnight, then ground and sieved to <125 μm. Illinois No. 6 coal was available in-house with a particle size <44 μm. Between 5 and 10 g of each blend (90:10, 80:20, 50:50 coal/BSG by mass) were made by measuring the desired mass of each fuel to the 0.1 mg on a Shimadzu semi-mircobalance into a glass vial and mechanically agitating with a Scilogex vortex mixer. Ultimate analyses of each of these materials are given in Table 1.

2.2. Thermogravimetric analysis

The pyrolysis and oxidation kinetic measurements were performed on a Mettler Toledo TGA/DSC1, with data output from Mettler STARe Default DB V10.00 software. The mass was logged every second to the 10^{-8} g, along with time and temperature to ±0.1 K. Between 7 and 12 mg of each sample (pure biomass, pure coal, and three different blends) were placed in a 70 μl alumina crucible and thermally treated in a N_2 (pyrolysis) or air (oxidative) atmosphere, flowing at approximately 50 ml/min. The biomass samples were heated from 298 K to 383 K at 50 K/min, and held at 383 K for 60 min to remove any residual water. The temperature was ramped back down to 298 K at −10 K/min and held for 5 min. For the pure biomass samples, the temperature was increased to 1023 K at 100 K/min to simulate fast pyrolysis/oxidation (while maintaining experimental reproducibility) and held for 5 min to insure that the reactions were complete (reactions were all complete before this temperature was reached) as a terminal mass is critical to determining the kinetic parameters. The coal and the biomass–coal blends were pyrolyzed/oxidized in the TGA through the same process, but up to a temperature of 1173 K to ensure complete decomposition of the coal. Each thermal treatment was repeated a minimum of three times per sample to insure reproducibility.

There are several factors to consider when describing the reaction kinetics for the combustion of biomass with coal. To overcome potential heat and mass transfer limitations, much research on biomass/coal kinetics has been performed at slow heating rates (<10 K/min). However, this does not model the rapid combustion processes in an industrial coal boiler with heating rates up to 1000 K/min. In this study we employ a fast heating rate of 100 K/min to insure reproducibility within our data but expand available literature on the kinetics of thermochemical conversion processes. This is performed for both the pyrolysis and oxidation of BSG and BSG–coal blends; pyrolysis is often a rate-limiting step in combustion during which most volatiles are released from the solid fuel. It was observed by van de Velden et al. [26] that there are mass transfer limitations in the pyrolysis of larger particles as larger particles and higher heating rates cause a temperature gradient from the outside to the center of the particle; as such we elect to use very fine particles to mitigate potential mass transfer limitations within the

Table 1
Ultimate analyses of brewer's spent grain and Illinois No. 6 coal.

wt.% (dry)	Illinois No. 6 Coal	Brewer's spent grain
C	70.2	49.70
H	4.8	6.54
N	0.9	3.86
S	3.1	0.33
O	9.9	34.87
Ash	11.1	4.70
Moisture %	4.2	5.68

particle. Our laboratory has previously shown that there is no apparent effect of particle size (between 125–250 μm, 250–300 μm, and 300–500 μm) on activation energy [20].

To determine global kinetic parameters, we use the reaction rate constant method, widely used in determining the activation energy and pre-exponential factor of solid fuels. The extent of conversion, x, is defined as:

$$x = \frac{m_0\text{-}m_t}{m_0\text{-}m_f}. \quad (1)$$

m_0 is initial mass, m_t is mass at time t in seconds, m_f is mass at complete decomposition. The rate of reacted material is:

$$\frac{dx(t)}{dt} = k(1\text{-}x(t)). \quad (2)$$

The reaction rate constant is modeled by the Arrhenius equation, under a first order reaction rate assumption as:

$$k = Ae^{-\frac{E_a}{RT}}. \quad (3)$$

R is the universal gas constant and T is the absolute temperature. For non-isothermal experiments, k is solved for with β as the heating rate:

$$k = \beta\frac{dx(T)}{dT}/(1\text{-}x(T)). \quad (4)$$

From a plot of $\ln(k)$ vs. $1/T$, Ea (activation energy) and A (pre-exponential factor) may be calculated:

$$\ln(k) = \ln(A) - \frac{1}{T}\frac{Ea}{R}. \quad (5)$$

The maximum rate of decomposition is found from derivative thermogravimetric (DTG) curves, plotting dx/dt versus T; the maximum rate occurs as a peak where the slope equals zero.

2.3. Pyrolysis gas chromatography–mass spectroscopy

As a solid is devolatilized, its macromolecular structure is altered because of depolymerization, vaporization, and cross-linking of the solid matrix, which leads to aromatic ring rupture, evolution of gaseous products and tars, and the formation of a carbonaceous char. Simultaneous measurement of the thermal behavior and gas devolatilization products of coal pyrolysis are commonly performed by coupling TGA with either MS or Fourier Transform Infrared Spectroscopy (FTIR) in an inert atmosphere [27] or with a Curie Point Apparatus, as done in this work. We use a Shimadzu QP-2010 Plus gas chromatograph–mass spectrometer with quadruple MS with EI detection (GCMS) equipped with a Frontier Double-Shot Pyrolyzer (EGA/PY-GC 3030D) to explore the gaseous products of coal–biomass blends in an inert atmosphere, mimicking the conditions in the TGA [21].

The samples (pure and blends) were weighed into a stainless steel crucible (1.42 ± 0.12 mg per run) that is loaded in the pyrolyzer. When the pyrolyzer reaches the set point temperature, the sample cup was rapidly introduced into the furnace. A helium atmosphere was used for pyrolysis of samples under a flow of 62 ml/min with a SHRX1-5MS GC column of length 30 m with an inner diameter of 0.25 mm. In order to avoid introducing water into the MS from residual moisture in the biomass, the sample was initially heated to 383 K to drive off water [23]. The pure biomass, coal, and blend samples were then pyrolyzed to 1173 K at 100 K/min for consistency with the TGA experiments. Flash pyrolysis was also performed to mimic industrial situations for co-combusting in a coal-fired boiler. The volatiles evolved and pyrolyzed gasses were carried by the He through the column, which is heated to 573 K for 5 min. Compound evolution was determined for the highest 50 peaks by total chromatograph area. Assuming peak area is directly proportional to compound concentration, the area, normalized to sample size, was compared for each compound across each sample [28,29] to offer a semi-quantitative analysis of the impact of blend ratio on compound devolatilization.

3. Results and discussion

On a global level, results indicate that the pyrolytic and oxidative thermal degradation of BSG and coal blends proceeds at rates and energies roughly corresponding to the mass fraction of each solid fuel present in the blend, though by no means a simply "additive" trend. On a chemical level, however, the semi-quantitative data offered by the GC–MS presents a slightly different story, suggesting that the blending of BSG and coal may repress the formation of some aromatics and promote the formation of other compounds.

3.1. Rates of thermal decomposition

Across the literature we see that coal–biomass blends display increasing mass loss rates, as noted through derivative weight peaks, for thermal evolution profiles as the percentage of biomass increases at lower temperatures. The reverse is noted at higher temperature mass loss regimes. We confirm this trend, as seen in Figs. 1 and 2, DTG curves for the pyrolysis and oxidation of pure BSG, coal, and their blends heated at 100 K/min under N_2 and air. The peaks on the DTG curves correspond to the maximum rate of mass loss during thermal treatment.

During pyrolysis, the DTG evolution profile for BSG shows that there are two primary peaks at temperatures of 595 K and 642 K. Biagini et al. [30] report that the maximum rate of devolatilization for hemicellulose occurs at 572 K, cellulose at 627 K, and lignin at 634 K, though it is well documented that lignin decomposes over a wider temperature range [9]. It is supposed that the two primary DTG peaks correspond to the decomposition of hemicellulose and cellulose fractions of the BSG for the lower and higher temperature peak, respectively, with lignin and other minimal BSG components (sugar, proteins, representing less than 10% of total mass) decomposing across the temperature profile [31]. The pyrolysis of pure Illinois No. 6 coal shows a primary DTG peak at 740 K. As the proportion of biomass increases in the blend, the heights of the peak—and thus the rate of conversion—increases fairly linearly and rather quickly at the lower temperature decomposition realm around 590 K. As seen in Fig. 3, the opposite trend appears at 740 K. That is, as the proportion of biomass increases the peak mass loss rate decreases, though not as abruptly as the differences at 590 K. As Vuthaluru [3] found during the co-pyrolysis of wheat straw and coal, our results suggest no obvious synergistic effects during the pyrolysis of coal–biomass blends in terms of overall conversion rates at peak temperatures.

As seen in Fig. 4, the linear or "additive" nature of mass loss rates with respect to BSG/coal proportion seen for pyrolysis at 100 K/min does not hold for oxidation at 100 K/min. While the DTG peak for the oxidation of each fuel and their blends all occurred around 580 K, a sharp decrease in peak mass loss rate is seen as the percent of BSG increases from 0 wt.% to 20 wt.%, at which point the decrease in peak mass loss rate is considerably less sharp as the percentage of BSG increases from 20 wt.% to 100 wt.%.

3.2. Apparent activation energies—pyrolysis

Many kinetic studies of biomass and coal pyrolysis show a reaction order of decomposition close to one; it is common in the literature to apply this global or apparent reaction order to account for all the reactions occurring simultaneously [32,33]. The data presented here show high degrees of linearity for each mass loss regime when graphed in an Arrhenius plot (as seen in Fig. 5), providing a reasonable basis for comparison to other first order thermal decompositions presented in

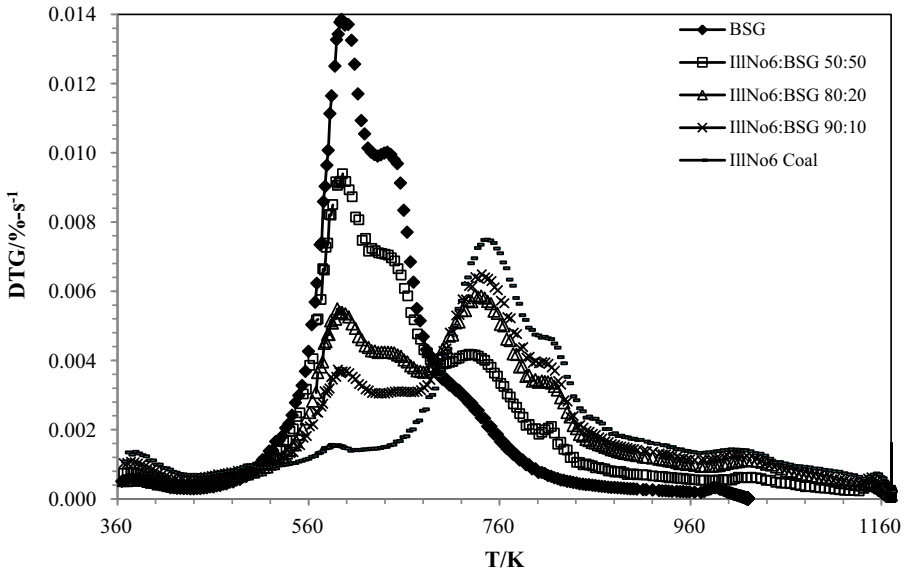

Fig. 1. DTG curves for the pyrolysis of BSG, Illinois No. 6 coal, and their blends at a heating rate of 100 K/min.

the literature. For lignocellulosic biomass there exist distinct thermal events during pyrolysis corresponding roughly to the decomposition of cellulose, hemicellulos, and lignin [34,35]. In the coal–biomass blends investigated here, we see four distinct activation energies of pyrolytic decomposition for the BSG, and five for the coal-BSG blends and coal. As seen in Table 2, the largest mass loss during pyrolysis for the BSG occurs roughly between 550 and 750 K, for the coal between 650 and 1025 K, and for the blends between 500 and 1025 K. The total amount of mass lost in the first mass loss regime (between ~425-550 K) is minimal—less than 2 wt.% for the blends and coal, suggesting that the nature of this step is an energy-intensive activation step, as opposed to the physical breaking of bonds and devolatilizing of compounds at this temperature (Fig. 6). The activation energies determined here align well with the kinetic constants presented by Pantoleontas et al. [35], who also find five decomposition fractions for a lignite coal and four for biomass samples. Like Pantoleontas et al., Vamvuka and co-workers [10,36] use this pure fuel data on a variety of biomass and lignite coal to predict co-firing characteristics, but do not measure the blended fuel kinetics.

As seen in Table 2 and Fig. 7, the first three temperature regimes for the pyrolysis of BSG and blends show activation energies that decrease substantially as the amount of biomass decreases. This is explained by the higher amounts of lignocellulosic material present in the biomass that decompose at lower temperatures (as compared to coal), which we already noted among the DTG curves. The fourth mass loss regime (higher temperature fraction; ~960 to 1025 K) shows increasing apparent activation energy with decreasing biomass content, and in the fifth mass loss regime, we see only the devolatilization of coal occurring; there appears to be little impact of the biomass on the trends in apparent activation energy. Biagini et al. [37] suggest that the weight loss curve of each blend is the sum of the weight loss curve of two coals (low and high volatile) and two biomasses (pine sawdust and sewage

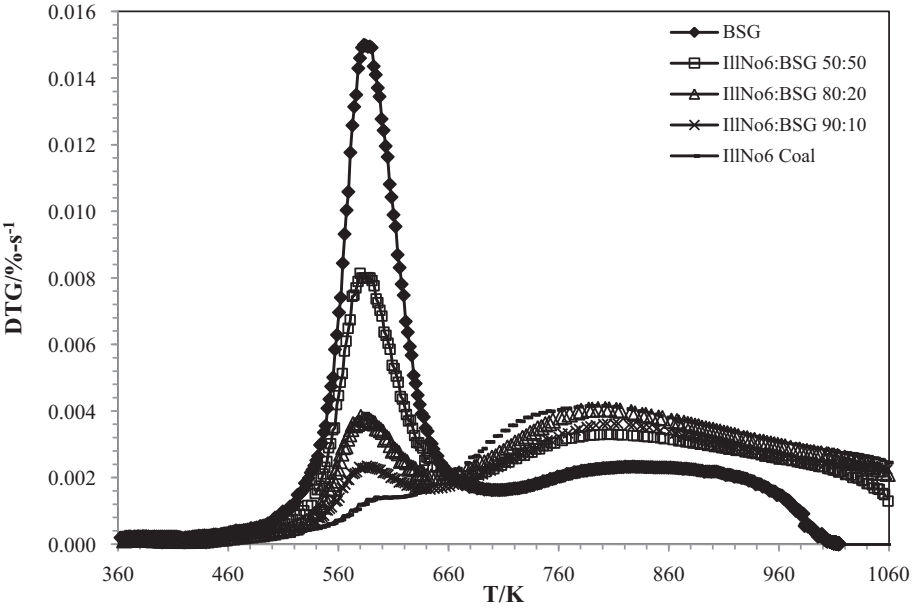

Fig. 2. DTG curves for the oxidation of BSG, Illinois No. 6 coal, and their blends at heating rate of 100 K/min.

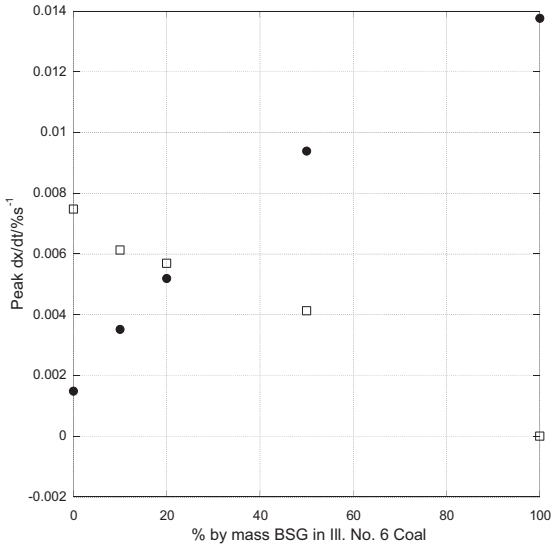

Fig. 3. Peak derivative mass loss rate for the pyrolysis of BSG, Illinois No. 6 coal, and their blends as a function of percent (by mass) BSG in Illinois No. 6 coal at (●) 590 K and (□) 740 K.

sludge) are the sum of the weight loss curves of each material. Furthermore, they find that kinetic parameters are, at least for a first estimate, well described by such assumptions. If we "predict" the activation energy for each mass loss regime as:

$$Ea_{predict} = y_{Coal}Ea_{Coal} + y_{BSG}Ea_{BSG} \quad (7)$$

where y is the mass fraction of coal and BSG (respectively) and Ea is the activation energy, we find evidence for reaction synergism beyond the non-linear behavior noted in Fig. 7. Fig. 8(a–d) shows the predicted versus measured activation energies as per Eq. (7) for mass loss regimes 1–4; there is no observed BSG decomposition in mass loss regime 5 and thus we cannot offer a predicted value (Table 3).

For mass loss regime 1, Eq. (7) predicts a value for the 10 wt.% BSG of 17.9 kJ/mol, and measure 17.3; for 20 wt.% predicted is 21.9 and measured 22.1. For the 50:50 blend, the predicted value is substantially higher (34.1 kJ/mol) than the measured value (19.6 kJ/mol), and the fraction mass lost in this range (2% by mass) is the same as the coal and other blends, as compared to 5% by mass for pure BSG, suggesting that the biomass pyrolysis may be suppressed by the presence of the coal, as the BSG pyrolysis activation energy in this temperature range is 54.2 kJ/mol. In mass loss regime 2, the predicted values are all significantly lower than the measured values; given that a substantial amount of biomass (15% by mass for pure BSG, 10% for 50:50 blend, 4% for 80:20 and 3% for 90:10, as compared to 1% for coal) is lost in this regime, we suspect a higher amount of the devolatilization products originating from the biomass in the blends, as opposed to the coal. In mass loss regime 3 the agreement between predicted and measured activation energies for the 50:50 and 90:10 blends are within one standard deviation of the measured values, though the Ea for 80:20 blend is about 30% lower than the predicted value. In regime 4 the predicted values are again higher than the measured values, suggesting that much of the biomass has preferentially devolatilized before reaching this temperature, as in this temperature range the activation energy for the coal pyrolysis is substantially higher than the BSG (90.3 versus 16.4 kJ/mol). Given behavior noted in regimes 1 and 2, this is likely a factor of a blend with significantly different composition (primarily coal) than the original 50, 20 or 10 wt.% BSG. The data presented in these tables and figures are the average of three experimental runs; the results from each run (for both pyrolysis and oxidation) are given in the Supplemental Information (available online).

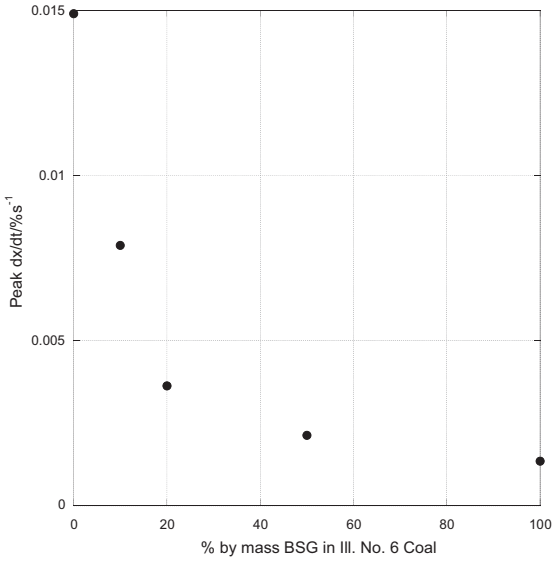

Fig. 4. Peak derivative mass loss rate for the oxidation of BSG, Illinois No. 6 coal, and their blends as a function of percent (by mass) BSG in Illinois No. 6 coal at 580 K.

3.3. Apparent activation energies—oxidation

The oxidation of the samples occurs over fewer steps than the pyrolysis. There are three mass loss regimes corresponding to primary oxidation of BSG, one of which results in only a 1% mass loss. There are four distinct steps of decomposition for the coal, though two of which result in only 1 and 2 wt.% decomposition, indicating only two primary decomposition steps. For the blends we see an amalgam of these distinct mass loss regimes; the low temperature step (~430 to 515 K) results, like pyrolysis, in less than 2% sample mass loss. The percent mass lost in the second mass loss regime (~400 to 580 K) decreases substantially as the percent of biomass decreases, as does the apparent oxidation energy, indicating that this step is primarily the oxidation of the biomass.

Though the trend is not quite linear, there is a strong dependence of global activation energy on blend composition, as seen in Fig. 9. In the third mass loss regime again we see a decrease in fraction of sample lost as biomass content decreases, though the activation energies are relatively similar, all in the range of ~37 to 47 kJ/mol. In the fourth mass loss regime we see clear oxidation of the coal in the blend. At temperatures between 980 and 1080 K, the apparent activation energy for the 50:50 blend is ~209 kJ/mol, and for the 80:10, 90:10 and 100% coal samples Ea is approximately 243 kJ/mol for the oxidation of each sample, with increasing fractional mass lost as the percent coal increases. From the mass lost over each regime and corresponding changes in activation energy, it would appear that the oxidation of the blended fuel does occur in distinct steps for each solid fuel component, with the biomass possibly promoting some coal oxidation at lower temperatures as seen in mass loss regimes two and three (Fig. 10). However, each solid fuel appears to oxidize in two steps, likely corresponding to its oxidation of released volatiles followed by char oxidation at higher temperatures. The activation energies predicted via Eq. (7) support this conclusion; if the blends oxidized as a weight-averaged fuel, we would see $Ea_{predicted} = Ea_{measured}$, such that each plot in Fig. 11 showed points along the $y = x$ line. Rather, in oxidation regimes 1 and 2 the measured activation energies are significantly higher than the predicted values according to Eq. (7), and for regime 3 the measured activation energies are considerably lower than predicted. This suggests that the BSG is oxidized at lower temperatures, and coal undergoes in its own devolatilization and char oxidation steps at higher temperatures.

Gil et al. [5] found two combustion steps for pine sawdust, the first occurring at 200–360 °C where volatiles are released and burned, and

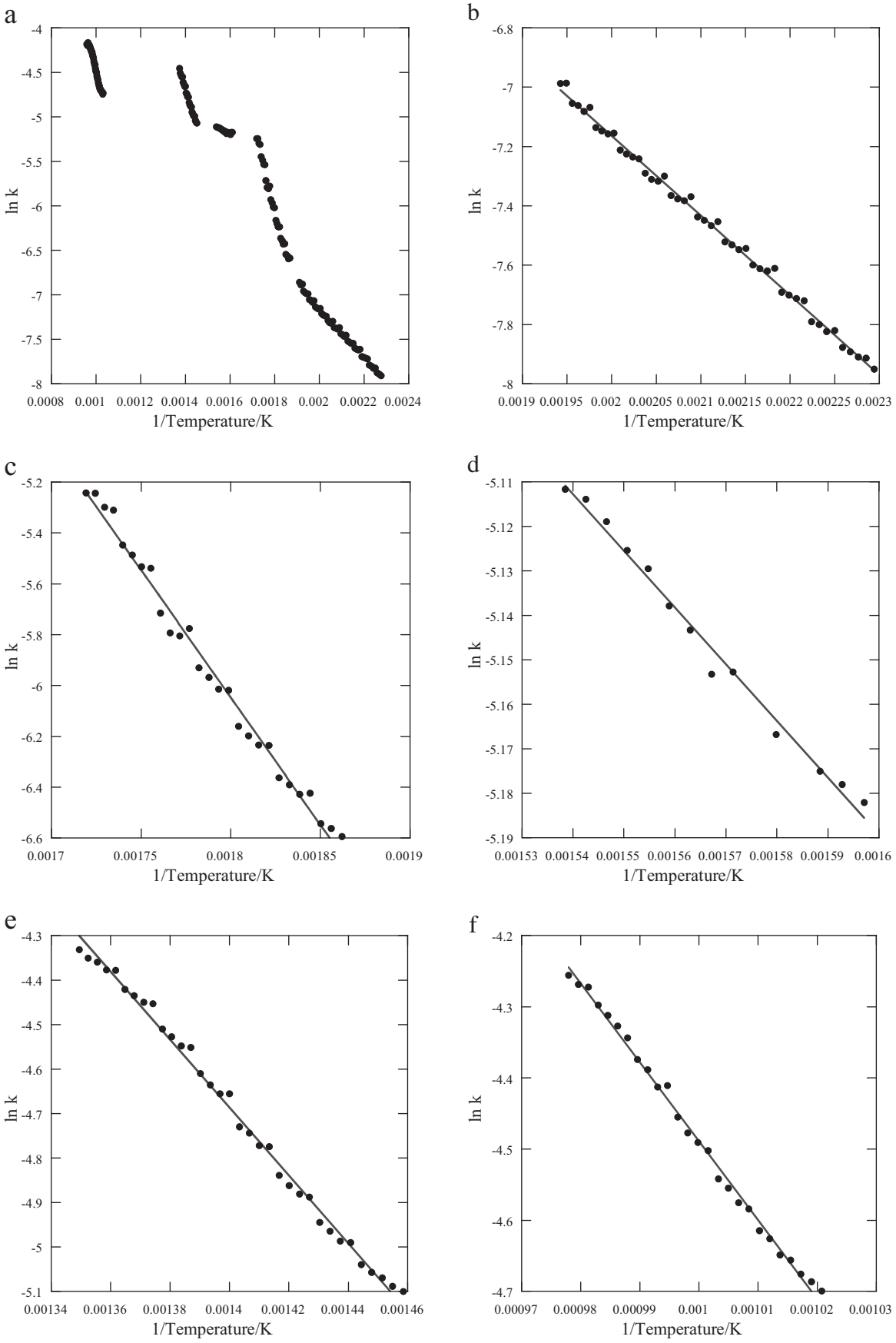

Fig. 5. Sample Arrhenius plot for pyrolysis of 20 wt.% BSG in Illinois No. 6 coal at 100 °C/min (a = full temperature range; b = mass loss regime 1; c = mass loss regime 2; d = mass loss regime 3; e = mass loss regime 4; f = mass loss regime 5).

Table 2
Average activation energies, pre-exponential factors, mass loss fractions and predicted activation energies according to Eq. (7) over a series of temperature-dependent mass loss regimes for pyrolysis of BSG–Illinois No. 6 coal blends.

	Onset temperature (K)	Endset temperature (K)	Activation energy (kJ/mol)	Pre-exponential factor (s^{-1})	Fraction sample mass loss	Predicted activation energy (kJ/mol)
Pyrolysis mass loss regime 1						
BSG	466.2 ± 5.9	547.0 ± 1.8	54.2 ± 3.0	2.72E + 02 ± 1.27E + 02	0.05 ± 0.01	
50:50 BSG/IllNo6	431.7 ± 0.9	496.8 ± 6.0	19.6 ± 0.6	8.29E−02 ± 1.13E−02	0.02 ± 0.01	34.1
20:80 BSG/IllNo6	428.1 ± 4.6	517.4 ± 7.2	22.1 ± 1.1	1.62E−01 ± 4.09E−02	0.02 ± 0.003	21.9
10:90 BSG/IllNo6	430.0 ± 2.0	524.6 ± 4.3	17.3 ± 2.9	6.13E−02 ± 3.14E−02	0.02 ± 0.01	17.9
IllNo6 coal	426.8 ± 5.6	530.5 ± 2.9	13.9 ± 1.2	2.51E−02 ± 5.22E−03	0.02 ± 0.002	
Pyrolysis mass loss regime 2						
BSG	550.4 ± 1.8	594.2 ± 2.4	105.2 ± 1.9	2.05E + 07 ± 7.29E + 06	0.15 ± 0.01	
50:50 BSG/IllNo6	503.8 ± 0.5	593.1 ± 1.2	92.5 ± 2.3	1.81E + 06 ± 9.84E + 05	0.10 ± 0.01	67.1
20:80 BSG/IllNo6	525.3 ± 7.4	587.6 ± 5.1	80.2 ± 1.3	8.53E + 04 ± 2.14E + 04	0.04 ± 0.01	44.2
10:90 BSG/IllNo6	534.8 ± 1.7	589.0 ± 2.7	61.2 ± 2.5	1.20E + 03 ± 6.89E + 02	0.03 ± 0.01	36.6
IllNo6 coal	544.5 ± 4.8	580.5 ± 3.9	29.0 ± 2.7	7.78E−01 ± 4.82E−01	0.01 ± 0.001	
Pyrolysis mass loss regime 3						
BSG	619.5 ± 4.6	654.5 ± 5.5	42.6 ± 0.8	4.23E + 01 ± 5.98E + 00	0.24 ± 0.02	
50:50 BSG/IllNo6	614.5 ± 0.2	650.5 ± 6.0	23.8 ± 2.2	9.83E−01 ± 5.21E−01	0.09 ± 0.03	25.2
20:80 BSG/IllNo6	617.0 ± 1.3	652.8 ± 4.8	11.3 ± 0.2	4.93E−02 ± 8.90E−04	0.04 ± 0.01	14.8
10:90 BSG/IllNo6	623.6 ± 1.3	676.4 ± 6.8	11.5 ± 0.5	3.43E−02 ± 1.78E−03	0.04 ± 0.01	11.3
IllNo6 coal	599.5 ± 3.3	639.6 ± 1.2	7.8 ± 0.8	7.74E−03 ± 1.15E−03	0.01 ± 0.002	
Pyrolysis mass loss regime 4						
BSG	683.7 ± 2.0	738.8 ± 6.1	16.4 ± 1.4	2.57E−01 ± 7.14E−02	0.17 ± 0.02	
50:50 BSG/IllNo6	681.7 ± 2.1	755.7 ± 4.6	41.7 ± 1.1	1.29E + 01 ± 2.48E + 00	0.11 ± 0.01	53.3
20:80 BSG/IllNo6	681.0 ± 4.5	747.8 ± 2.9	64.3 ± 1.1	4.72E + 02 ± 8.09E + 01	0.10 ± 0.02	75.5
10:90 BSG/IllNo6	686.8 ± 5.4	744.4 ± 4.9	77.0 ± 1.9	3.68E + 03 ± 1.15E + 03	0.11 ± 0.05	82.9
IllNo6 coal	646.0 ± 6.0	745.6 ± 7.2	90.3 ± 3.3	3.34E + 04 ± 1.67E + 04	0.09 ± 0.01	
Pyrolysis mass loss regime 5						
BSG						
50:50 BSG/IllNo6	966.3 ± 4.5	1015.7 ± 10.1	73.3 ± 4.3	8.80E + 01 ± 7.45E + 01	0.09 ± 0.04	
20:80 BSG/IllNo6	973.4 ± 9.4	1022.1 ± 10.5	94.4 ± 3.1	1.00E + 03 ± 3.34E + 02	0.07 ± 0.01	
10:90 BSG/IllNo6	961.2 ± 1.1	1023.1 ± 18.4	84.1 ± 1.9	2.91E + 02 ± 6.74E + 01	0.08 ± 0.03	
IllNo6 coal	965.2 ± 4.8	1025.3 ± 13.6	75.4 ± 2.4	1.07E + 02 ± 2.87E + 01	0.08 ± 0.02	
Overall pyrolysis total mass loss						
BSG					0.74 ± 0.005	
50:50 BSG/IllNo6					0.56 ± 0.04	
20:80 BSG/IllNo6					0.44 ± 0.001	
10:90 BSG/IllNo6					0.38 ± 0.02	
IllNo6 coal					0.35 ± 0.004	

the second at 360–490 °C corresponding to char oxidation. Using an overall, or apparent, first order reactions scheme for the oxidation of coal–biomass blends, they determined that the co-combustion of pine sawdust with coal shows no synergistic reaction effects and that the first step for the oxidation of biomass and coal combustion may be modeled by first order kinetics. However, their activation energies

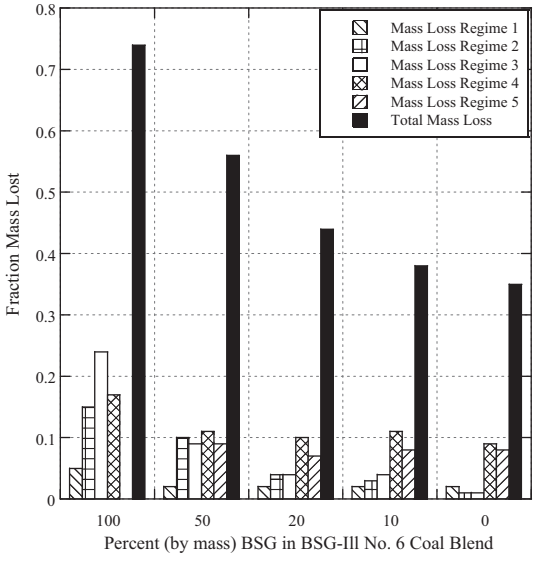

Fig. 6. Fraction of mass lost over each mass loss regime and fraction of total sample mass lost for each fuel and blend during pyrolysis.

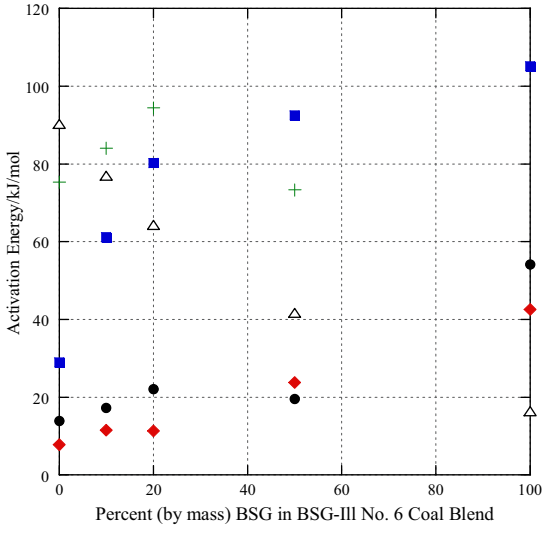

Fig. 7. Activation energy of pyrolysis as a function of percent, by mass, BSG in mixture (●) mass loss regime 1; (■) mass loss regime 2; (◆) mass loss regime 3; (Δ) mass loss regime 4; (+) mass loss regime 5.

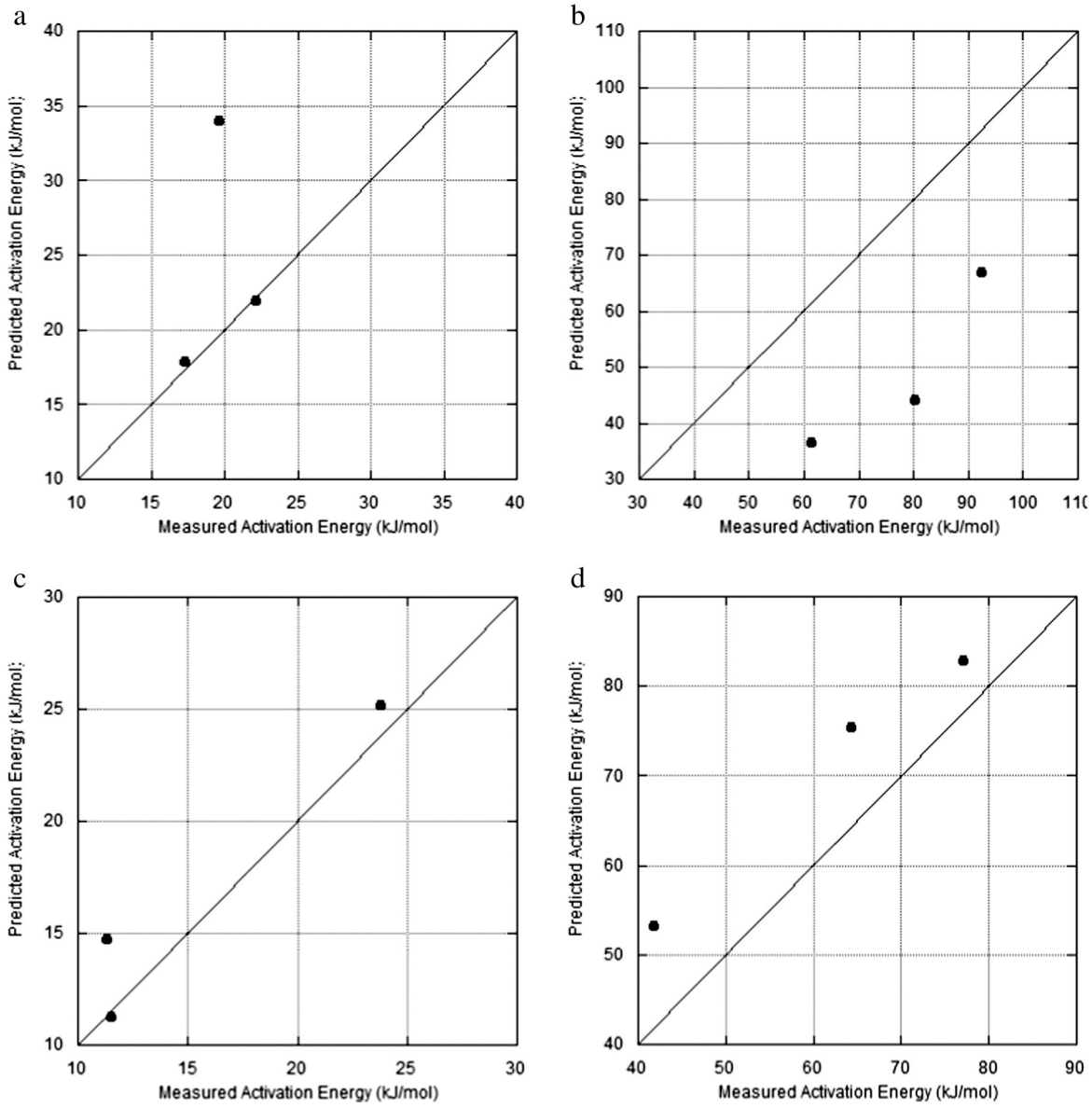

Fig. 8. Predicted activation energy of pyrolysis via Eq. (7) versus measured activation energy of pyrolysis for each blend for (a) mass loss regime 1; (b) mass loss regime 2; (c) mass loss regime 3; (d) mass loss regime 4.

over the two stages are considerably higher than ours determined here; for 10% pine sawdust in coal, they find an *Ea* of 149.5 kJ/mol for the first decomposition region and 115.8 kJ/mol over the second, as compared to our 88.2 and 37.3 kJ/mol, respectively. Sahu et al. [38] report activation energies for the combustion of a medium volatile coal and saw dust blends ranging from 32.8 to 125.3 kJ/mol and of the same coal and rice husk from 25.2 to 105.3 kJ/mol.

In this study the apparent oxidation activation energy for the first two mass loss regimes decreases as the BSG content decreases in BSG-Illinois No. 6 coal blends. The opposite occurs when comparing values for the higher temperature mass loss regime, where the apparent activation energy increases with increasing coal content. The same was noted at higher temperatures during pyrolysis, with thermal degradation steps dependent on the sum of components in the blends. However, the activation energies required for the thermal degradation of BSG + IllNo6 coal blends—via oxidation or pyrolysis—are not simply an "additive" function according to blend composition. We explore this further through a look at the devolatilization profiles of blends via Py–GC–MS.

3.4. Devolatilization profile of blends

The thermal desorption of volatiles from biomass occurs at relatively low temperatures during pyrolysis. Aromatic hydrocarbons are formed when pyrolyzing cellulose due to reactions at higher temperatures [39]. The pyrograms for rapid pyrolysis (100 K/min) show that many aromatic compounds, such as phenols and benzenes, are present in the pyrolysis gases of all samples. Heavy hydrocarbons (C_{14}^{+}) are also present in the BSG and blends. Fig. 12 compares the chromatograph area percent of a series of compounds detected through the Py–GC–MS experiments. Figures S1–S4 (available in online supplemental material) show plots of these compounds as a function of weight percent of BSG in the BSG–IllNo6 coal blend. The inclusion of biomass appears to significantly decrease/suppress the formation of some compounds, such as the phenols detected here; 2-methyl phenol decreases linearly and rapidly as the BSG is added to the blend, whereas the 2,5-dimethyl phenol decreases exponentially as the percentage of BSG increases, as seen in Table 4. At 50 wt.% BSG we see no 2-methyl phenol, and at

Table 3
Average activation energies, pre-exponential factors, mass loss fractions and predicted activation energies according to Eq. (7) over a series of temperature-dependent mass loss regimes for oxidation of BSG–Illinois No. 6 coal blends.

	Onset temperature (K)	Endset temperature (K)	Activation energy (kJ/mol)	Pre-exponential factor (s^{-1})	Fraction sample mass loss	Predicted activation energy (kJ/mol)
Oxidation mass loss regime 1						
BSG	428.0 ± 8.2	482.8 ± 0.9	28.0 ± 1.5	0.56 ± 0.2	0.01 ± 0.004	
50:50 BSG/IllNo6	426.8 ± 6.5	489.5 ± 11.7	37.2 ± 1.8	3.76 ± 1.6	0.01 ± 0.003	22.3
20:80 BSG/IllNo6	432.7 ± 3.2	489.2 ± 19.1	30.7 ± 1.3	0.61 ± 0.2	0.01 ± 0.001	18.8
10:90 BSG/IllNo6	440.4 ± 9.0	516.3 ± 4.8	20.9 ± 2.7	0.06 ± 0.03	0.02 ± 0.000	17.7
IllNo6 coal	438.6 ± 8.7	488.6 ± 3.8	16.5 ± 2.5	0.02 ± 0.01	0.01 ± 0.001	
Oxidation mass loss regime 2						
BSG	498.4 ± 7.6	582.1 ± 2.4	129.8 ± 2.0	1.04E + 10 ± 5.49E + 09	0.21 ± 0.01	
50:50 BSG/IllNo6	507.5 ± 10.7	577.6 ± 1.3	127.2 ± 5.6	4.66E + 09 ± 4.35E + 09	0.09 ± 0.02	92.5
20:80 BSG/IllNo6	522.5 ± 2.9	571.9 ± 4.4	105.6 ± 4.8	2.26E + 07 ± 1.79E + 07	0.04 ± 0.002	70.1
10:90 BSG/IllNo6	523.9 ± 0.9	575.3 ± 3.8	87.6 ± 3.5	2.47E + 05 ± 1.45E + 05	0.03 ± 0.002	62.6
IllNo6 coal	523.6 ± 8.4	581.2 ± 3.1	55.1 ± 5.1	1.56E + 02 ± 1.62E + 02	0.02 ± 0.003	
Oxidation mass loss regime 3						
BSG	681.6 ± 6.8	976.0 ± 21.8	40.6 ± 0.7	3.82 ± 1.2	0.45 ± 0.1	
50:50 BSG/IllNo6	669.8 ± 5.5	929.2 ± 11.6	36.9 ± 3.0	1.73 ± 0.6	0.23 ± 0.03	43.6
20:80 BSG/IllNo6	657.4 ± 13.2	940.2 ± 11.2	37.0 ± 5.3	2.84 ± 0.7	0.16 ± 0.04	45.4
10:90 BSG/IllNo6	654.0 ± 1.5	983.7 ± 1.4	39.7 ± 2.6	2.72 ± 1.1	0.15 ± 0.01	46.0
IllNo6 coal	621.3 ± 6.2	967.0 ± 3.3	46.6 ± 1.2	9.05 ± 2.1	0.16 ± 0.01	
Oxidation mass loss regime 4						
BSG						
50:50 BSG: IllNo6	980.7 ± 13.3	1052.3 ± 9.6	208.7 ± 15.9	6.44E + 08 ± 6.47E + 07	0.33 ± 0.1	
20:80 BSG/IllNo6	1042.8 ± 2.7	1087.6 ± 0.7	243.7 ± 5.3	8.05E + 10 ± 4.35E + 10	0.45 ± 0.0	
10:90 BSG/IllNo6	1023.9 ± 9.7	1084.7 ± 6.2	242.6 ± 10.6	3.89E + 10 ± 2.10E + 10	0.48 ± 0.02	
IllNo6 coal	1015.6 ± 5.8	1085.7 ± 11.0	242.8 ± 3.9	1.50E + 10 ± 3.41E + 09	0.59 ± 0.04	
Overall oxidation total mass loss						
BSG					0.91 ± 0.003	
50:50 BSG/IllNo6					0.81 ± 0.004	
20:80 BSG/IllNo6					0.78 ± 0.0	
10:90 BSG/IllNo6					0.78 ± 0.01	
IllNo6 coal					0.83 ± 0.03	

80 wt.% BSG we see no 2,5-dimethyl phenol. Similarly, heneicosane, 1-tridecane and undecane decrease as the weight percent of BSG increases. The opposite trend holds for *n*-hexadecanoic acid; we detect none in the pure coal and 10 wt.% BSG blend, but see increasing amounts at 20 wt.%, 50 wt.% and pure BSG. There are no clear trends for some compounds, such as octadecanoic acid and heptadecane, as a function of %BSG. However, hexadecane appears only in the pure BSG, not in any of the blends. The total amount of naphthalenes present—polycyclic aromatic compounds—decreases substantially and non-additively as the amount of BSG increases in the blend (none were detected in the BSG). This is not surprising; these compounds are known to be by-products of fossil fuel decomposition reactions.

The GC–MS work on the blends here was performed at heating rates of 100 °C/min to mimic the TGA experimental work. We note an important effect of heating rate on devolatilizing compounds

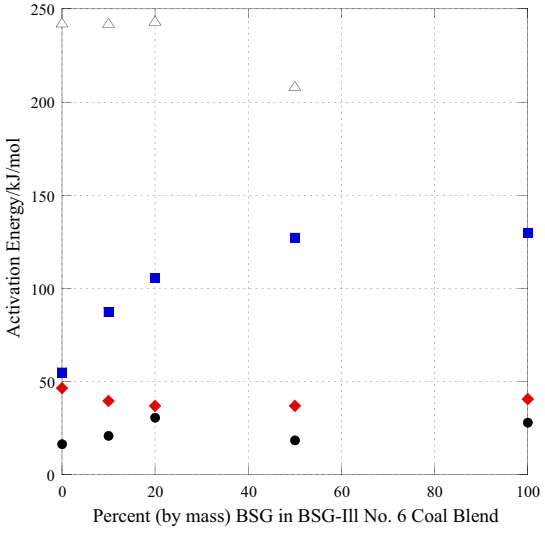

Fig. 9. Activation energy of oxidation as a function of percent, by mass, BSG in mixture: (●) mass loss regime 1; (■) mass loss regime 2; (◆) mass loss regime 3; (△) mass loss regime 4.

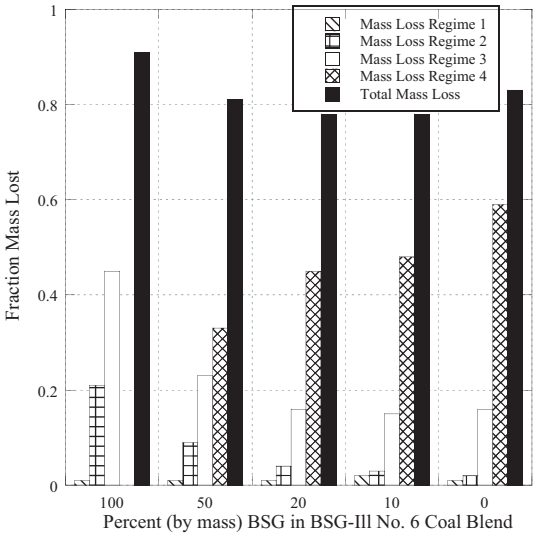

Fig. 10. Fraction of mass lost over each mass loss regime and fraction of total sample mass lost for each fuel and blend during oxidation.

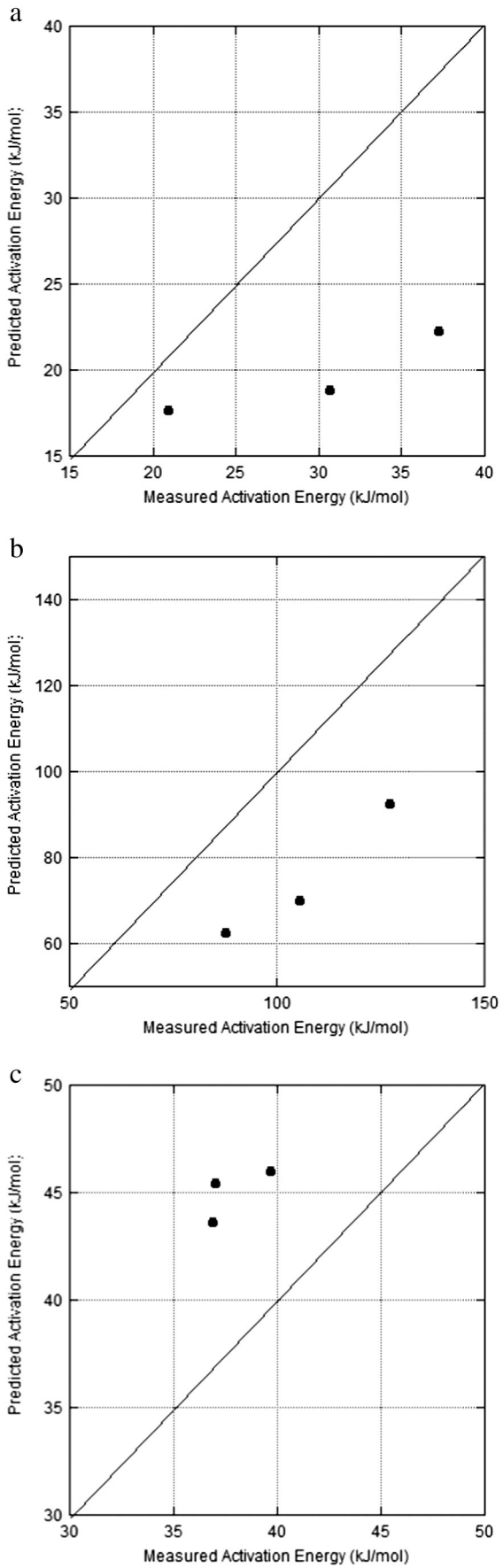

Fig. 11. Predicted activation energy of oxidation via Eq. (7) versus measured activation energy of pyrolysis for each blend for (a) mass loss regime 1; (b) mass loss regime 2; and (c) mass loss regime 3.

through subsequent GC–MS experiments; though previous work in our laboratory shows little effect of heating rate (between 10 and 100 K/min) on the pyrolysis of some hemicellulosic biomass [20], clearly there are differences in the chemical reactions occurring during pyrolysis at different heating rates/residence times. Fig. 13 compares the area percent of selected aromatics across different heating rates found in the pyrolysis of IllNo6 coal in order to compare relative yields, as done by González-Vila et al. [28]. The identifiable aromatics evolved consisted of naphthalenes, benzene rings, toluene, phenol, and anthracene, common byproducts of the incomplete combustion of carbonaceous fuels. When we increase the heating rate to flash pyrolysis, the amount of phenols volatilizing decreased and the concentration of benzene increased. During flash pyrolysis, only toluene and anthracene were identified in the gaseous products. The immediate addition of high heat to the particles may have caused critical bonds to be weakened for the release of these compounds. Fig. 14 compares the area percent of organic acids evolved during the pyrolysis of BSG at different heating rates. The only organic acid present during flash pyrolysis is acetic acid, 2-ethylhexyl ester at 1.2% by area. At low heating rate, formic acid evolved (1.2% by area), and acetic acid evolved at increasing concentrations with heating rates; these compounds are known to form from cellulose pyrolysis [39]. Sanna et al. study the pyrolysis of spent grain pyrolysis over activated alumina and find lighter compound yields increasing with increasing temperature, similar to the impact we note in increasing heating rate [40]. Because compounds appear at different concentrations in blends that are not necessarily an additive function of coal/biomass composition, we suspect that possible synergistic reactions may be occurring on a molecular level [21].

3.5. Summary: Additive versus synergistic behavior

There is much debate in the literature concerning the additive versus synergistic nature of thermochemical conversions of coal–biomass blends, specifically during pyrolysis. Krerkkaiwan et al. [41] suggest that this disagreement may be an artifact of operating parameters (temperature, pressure, heating rate, fuels, blend ratio and type of experiment). They suggest that the slow (~10 °C/min) heating rate of conventional TGA experiments or short residence time of fluidized bed may explain the lack of synergistic effects. Using a drop tube fixed-bed reactor, Krerkkaiwan et al. demonstrate synergism between a subbituminous coal and two biomasses (rice stream and *Leucaena leucocepha* wood), suggesting that a larger amount of H and OH radicals from the biomass may catalyze cracking of aromatic compounds in the coal, and that alkali and alkaline earth metals present may increase char reactivity and gasification. Sonobe et al. [42] find no evidence of synergism in their TGA experiments, though they do see synergistic reactions in the pyrolysis products of lignite/corncob pyrolysis in a fixed-bed reactor. Likewise, Kastanaki et al. [43] report no synergistic interactions in the solid phase between a Greek lignite coal and four biomasses (two olive mill wastes and a forest and cotton residue). Interestingly, Sanna et al. [44] find that oxidation of blends of bituminous coal and chars remaining after wheat spent grain and rapeseed meal pyrolysis display similar behavior; at lower temperatures the biochar has an initial release of volatiles below 400 °C, following a fairly additive trend up to 700 °C, at which point the at 10 wt.% bio-char blend showed slower converstion than coal alone. They suggest this is likely due to "interaction between the coal and the bio-coke during the final stages of oxidation in the TGA."

Given that we see both additive (in terms of peak mass loss rates and temperatures) and synergistic (in terms of activation energies and devolatilization profiles) behavior for the same set of fuel blends across different experiments, we note a further conclusion: globally, the energy required to initiate pyrolysis is somewhat dependent on the percent of biomass present in the blend, whereby each fuel impacts the activation energy as a function of its concentration, but not through a simple additive function. The possibility of synergistic reactions occurring at

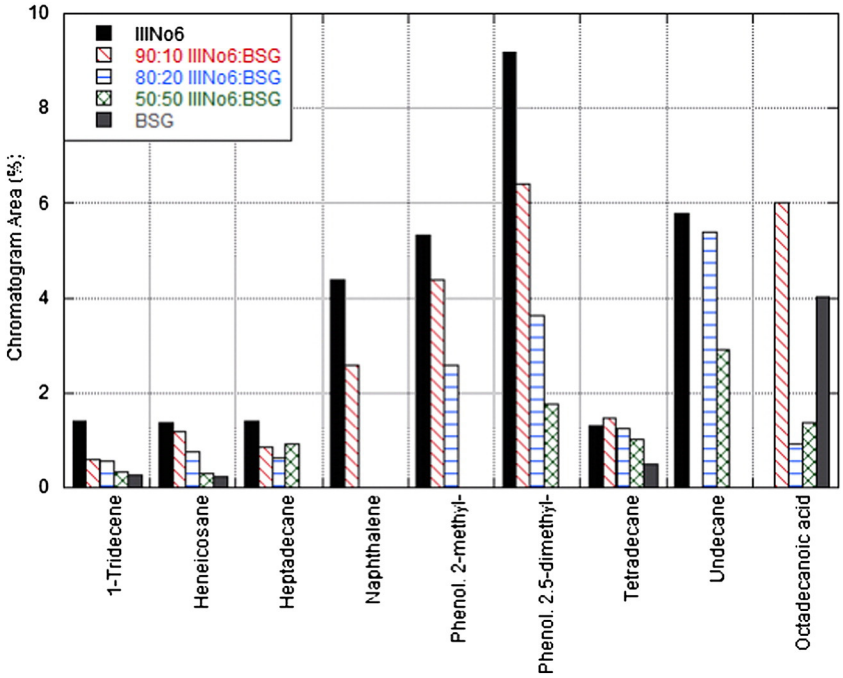

Fig. 12. Percent of chromatogram area of select compounds detected in rapid pyrolysis of Illinois No. 6 coal, BSG and blends at 100 °C/min (solid black = IllNo6; diagonal red = 90:10 IllNo6/BSG; horizontal blue = 80:20 IllNo6/BSG; cross-hatch green = 50:50 IllNo6/BSG; solid gray = BSG).

molecular level that are not reflected in global reaction kinetics may potentially be due to a pseudo-catalytic effect between the coal and biomass particles. That is, at a molecular level, the addition of biomass to coal may promote or suppress the formation of some compounds. This is analogous to work performed by Sanna et al. [40] on both wheat and barley spent grains. They show that the bio-fuel yield and compositions can be altered by pyrolyzing the biomass in fluidized beds with activated alumina, which lowers bio-oil nitrogen and oxygen contents, increasing stability and increasing O and N retention in the chars. Further work by this group finds that using activated serpentine and olivine led to higher levels of aliphatics and hydrogen, improving the energy yield in bio-oil conversion, attributed to macromolecules in the oxygenated bio-oil interacting with active sites of the catalyst [45]. We suspect a similar type of behavior when the BSG interacts with the coal surface and devolatilization products; the inorganic content of the coal may promote similar catalytic activity, leading to different products formed. However, from our and literature data it is not clear if the synergistic nature of the decomposition products is due to primary devolatilization or secondary reactions occurring in the vapor phase.

4. Conclusions

The present work explores the pyrolysis and oxidation behavior of brewer's spent grains and Illinois No. 6 coal blends at a fast heating rate of 100 K/min using thermogravimetric analysis and pyrolysis–gas chromatography–mass spectroscopy. Derivative thermogravimetric curves show that the rates of devolatilization of BSG and IllNo6 coal and their blends are a function of the amount of each solid fuel present, but this is not the case for oxidation. As sharp decrease in mass loss rate is observed as the percentage of BSG increases from 0 to 20%. The apparent, or global activation energies of pyrolysis are well represented by a first order Arrhenius plot with different activation energies for each mass loss regime over consistent temperature ranges. The energy required to pyrolyze the BSG–coal blends in each mass loss regime is not an additive function of each fuel's contribution to the blend. Rather, at lower temperatures the biomass appears to preferentially devolatilize, and at high temperatures a higher proportion of coal remains in the blends, contributing to higher activation energy than would be predicted by a simple additive scheme, likely due simply

Table 4
Percent by area of selected compounds detected in Py–GC–MS chromatograms as a function of blend ratio pyrolyzed at 100 °C/min.

Compound	Start RT (min)	End RT (min)	ILLNo6 (Area %)	90:10 (Area %)	80:20 (Area %)	50:50 (Area %)	BSG (Area %)
1-Tridecene	39.500	39.550	1.41	0.60	0.55	0.34	0.25
Heneicosane	53.660	53.740	1.37	1.19	0.75	0.30	0.23
Heptadecane	44.665	44.725	1.41	0.86	0.62	0.92	
Naphthalene	38.025	38.100	4.38	2.57			
Phenol, 2-methyl-	35.935	36.060	5.34	4.38	2.59		
Phenol, 2,5-dimethyl-	37.490	37.665	9.20	6.41	3.63	1.78	
Tetradecane	40.990	41.060	1.32	1.46	1.25	1.02	0.48
Undecane	36.410	36.505	5.80		5.38	2.90	
Octadecanoic acid	49.430	49.575		6.01	0.93	1.36	4.02
n-Hexadecanoic acid	47.545	47.710			11.26	19.00	22.89
Hexadecane	39.595	39.690					0.25
Acetic acid, 2-ethylhexyl ester	36.205	36.325					0.83
Total naphthalenes			13.98	9.27	2.48	1.08	

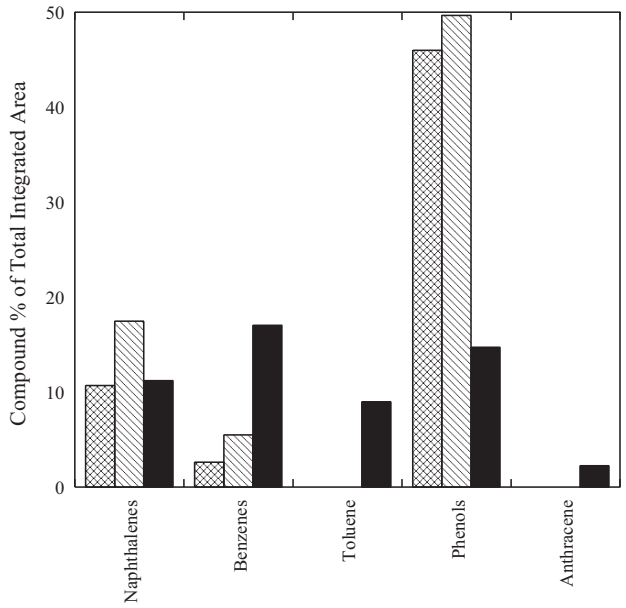

Fig. 13. Selected aromatic compounds detected in pyrolysis of IllNo6 coal at heating rates of 50 °C/min (crosslinks), 100 °C/min (diagonal), and flash pyrolysis (solid).

to changing concentrations of coal in the blend as biomass leaves the mixture. Likewise, for the oxidation of BSG–coal blends, while the thermal decomposition occurs over one fewer mass loss regime, the activation energies are again not an additive function of each fuels' contribution. There is a strong dependence of global activation energy on the composition of the whole, but it is not a linear function. As the BSG content decreases, so does the apparent oxidation activation energy at low temperatures, and vice versa. Curie point analysis of the solid fuels and blends shows that some compounds devolatilize in a manner somewhat proportional to each fuel, whereas others, such as the methylated phenols, are suppressed by the inclusion of biomass into the blends.

The implications of this work are twofold: first, it suggests that simple "back of the envelope" calculations that predict the pyrolysis and oxidation behavior of some biomass–coal blends based solely on a mass-fraction weighted contribution of each fuel are likely to both over- and under-predict energy required to initiate thermal decomposition depending on the temperature regime. Second, this finding, in conjunction with the non-additive behavior noted through specific compound evolution, suggests reaction synergism between some biomass–coal blends that may have broader-reaching consequences for co-firing in coal boilers in terms of the formation of hazardous air pollutants.

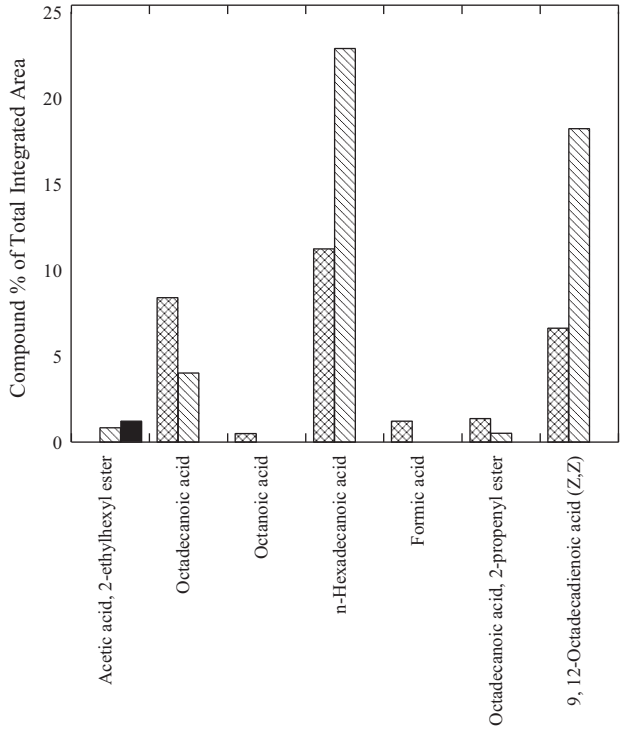

Fig. 14. Selected organic acids found during pyrolysis of BSG at heating rates of 50 °C/min (crosslinks), 100 °C/min (diagonal), and flash pyrolysis (solid).

Acknowledgments

Joe Thorner of Redhook Brewery, Portsmouth, NH, is acknowledged for providing the spent brewer's grain for this investigation. The authors thank Pablo Yangali for running additional Py–GC–MS experiments. This material is based upon work supported by the National Science Foundation under Grant No. NSF CBET-1127774.

Appendix A. Supplementary data

Supplementary data to this article can be found online at http://dx.doi.org/10.1016/j.fuproc.2014.08.004.

References

[1] A. Demirbas, Sustainable cofiring of biomass with coal, Energy Conversion and Management 44 (2003) 1465–1479.
[2] M. Díaz-Somoano, S. Unterberger, K. Hein, Prediction of trace element volatility during co-combustion processes, Fuel 85 (2006) 1087–1093.
[3] H.B. Vuthaluru, Thermal behaviour of coal/biomass blends during co-pyrolysis, Fuel Processing Technology 85 (2003) 141–155.
[4] H. Haykiri-Acma, S. Yaman, Effect of co-combustion on the burnout of lignite/biomass blends: a Turkish case study, Waste Management 28 (2008) 2077–2084.
[5] M.V. Gil, D. Casal, C. Pevida, J.J. Pis, F. Rubiera, Thermal behaviour and kinetics of coal/biomass blends during co-combustion, Bioresource Technology 101 (2010) 5601–5608.
[6] W. de Jong, G. Di Nola, B. Venneker, H. Spliethoff, M. Wójtowicz, TG-FTIR pyrolysis of coal and secondary biomass fuels: determination of pyrolysis kinetic parameters for main species and NO_x precursors, Fuel 86 (2007) 2367–2376.
[7] D.K. Shen, S. Gu, K.H. Luo, A.V. Bridgwater, M.X. Fang, Kinetic study on thermal decomposition of woods in oxidative environment, Fuel 88 (2009) 1024–1030.
[8] S. Munir, W. Nimmo, B.M. Gibbs, Co-combustion of agricultural residues with coal: turning waste into energy, Energy & Fuels 24 (2010) 2146–2153.
[9] S.S. Idris, N.A. Rahman, K. Ismail, A.B. Alias, Z.A. Rashid, M.J. Aris, Investigation thermochemical behaviour of low rank Malaysian coal, oil palm biomass and their blends during pyrolysis via thermogravimetric anaysis (TGA), Bioresource Technology 101 (2010) 4584–4592.
[10] D. Vamvuka, E. Kakaras, P. Grammelis, Pyrolysis characteristics and kinetics of biomass residuals mixtures with lignite, Fuel 82 (2003) 1949–1960.
[11] M. Fernandez, J. Rodriguez, M. Garcia, I. Gracia, Application of supercritical fluid extraction to brewer's spent grain management, Industrial and Engineering Chemistry Research 47 (2008) 1614–1619.
[12] D.C. Elliott, Catalytic hydrothermal gasification of biomass, Biofuels, Bioproducts and Biorefining 2 (2008) 254–265.
[13] Z. Luo, S. Wang, Y. Liao, K. Cen, Mechanism study of cellulose rapid pyrolysis, Industrial and Engineering Chemistry Research 43 (2004) 7607–7610.
[14] W. Mérida, P.-C. Maness, R.C. Brown, D.B. Levin, Enhanced hydrogen production from indirectly heated, gasified biomass, and removal of carbon gas emissions using a novel biological gas reformer, International Journal of Hydrogen Energy 29 (2004) 283–290.
[15] D. Mohan, C.U. Pittman Jr., P.H. Steele, Pyrolysis of wood/biomass for bio-oil: a critical review, Energy & Fuels 20 (2006) 848–889.
[16] P.K. Adapa, C. Karunakaran, L.G. Tabil, G.J. Schoenau, Qualitative and quantitative analysis of lignocellulosic biomass using infrared spectroscopy, Paper No. CSBE09-307. CSBE/SCGAB 2009 Annual Conference, The Canadian Society for Bioengineering, Prince Edward Island, Canada, 2009, (Accessed 10/10/2013. Available at: http://www.csbe-scgab.ca/docs/meetings/2009/CSBE09307.pdf).
[17] N. Prakash, T. Karunanithi, Kinetic modeling in biomass pyrolysis—a review, Journal of Applied Sciences Research (2008) 1627–1636.
[18] H. Yang, R. Yan, H. Chen, D.H. Lee, C. Zheng, Characteristics of hemicellulose, cellulose and lignin pyrolysis, Fuel 86 (2007) 1781–1788.

[19] P. Grammelis, P. Basinas, A. Malliopoulou, G. Sakellaropoulos, Pyrolysis kinetics and combustion characteristics of waste recovered fuels, Fuel 88 (2009) 195–205.
[20] L. Buessing, J.L. Goldfarb, Energy along I-95: pyrolysis kinetics of Floridian cabbage palm (*Sabal palmetto*), Journal of Analytical and Applied Pyrolysis 96 (2012) 78–85.
[21] J.M. Jones, M. Kubacki, K. Kubica, A.B. Ross, A. Williams, Devolatilisation characteristics of coal and biomass blends, Journal of Analytical and Applied Pyrolysis 74 (2005) 502–511.
[22] A.K. Sadhukhan, P. Gupta, T. Goyal, R.K. Saha, Modelling of pyrolysis of coal–biomass blends using thermogravimetric analysis, Bioresource Technology 99 (2008) 8022–8026.
[23] M. Sami, K. Annamalai, M. Wooldridge, Co-firing of coal and biomass fuel blends, Progress in Energy and Combustion Science 27 (2001) 171–214.
[24] D.J. Aerts, K. Bryden, J.M. Hoerning, K.W. Ragland, Co-firing switchgrass in a 50 MW pulverized coal boiler, Proceedings of the 59th Annual, 59, American Power Conference, Chicago, IL, 1997, pp. 1180–1185.
[25] C.Y.H. Chao, P.C.W. Kwong, J.H. Wang, C.W. Cheung, G. Kendall, Co-firing coal with rice husk and bamboo and the impact on particulate matters and associated polycyclic aromatic hydrocarbon emissions, Bioresource Technology 99 (2008) 83–93.
[26] M. Van de Velden, J. Baeyens, A. Brems, R. Dewil, Fundamentals, kinetics and endothermicity of the biomass pyrolysis reaction, Renewable Energy 35 (2010) 232–242.
[27] A. Arenillas, F. Rubiera, J.J. Pis, Simultaneous thermogravimetric-mass spectrometric study on the pyrolysis behaviour of different rank coals, Journal of Analytical and Applied Pyrolysis 50 (1999) 31–46.
[28] F.J. González-Vila, P. Tinoco, G. Almendros, F. Martin, Pyrolysis–GC–MS analysis of the formation and degradation stages of charred residues from lignocellulosic biomass, Journal of Agricultural and Food Chemistry 49 (2001) 1128–1131.
[29] J.-Y. Liu, S.-B. Wu, R. Lou, Chemical structure and pyrolysis response of Beta-O-4 lignin model polymer, Bioresources 6 (2011) 1079–1093.
[30] E. Biagini, F. Barontini, L. Tognotti, Devolatilization of biomass components studied by TG/FTIR technique, Industrial and Engineering Chemistry Research 45 (2006) 4486–4493.
[31] A. Aboulkas, K. El harfi, A. El boudaili, M. Nadifiyine, M. Benchanaa, A. Mokhlisse, Pyrolysis kinetics of olive residue/plastic mixtures by non-isothermal thermogravimetry, Fuel Processing Technology 90 (2009) 722–728.
[32] C. Branca, C. Di Blasi, Kinetics of the isothermal degradation of wood in the temperature range 528–708 K, Journal of Analytical and Applied Pyrolysis 67 (2003) 207–219.
[33] P. Parasuraman, R. Singh, T. Bolton, S. Omori, R. Francis, Estimation of hardwood lignin concentrations by UV spectroscopy and chlorine demethylation, BioResources 2 (2007) 459–471.
[34] Q. Cao, K.-C. Xie, W.-R. Bao, S.-G. Shen, Pyrolytic behavior of waste corn cob, Bioresource Technology 94 (2003) 83–89.
[35] G. Pantoleontos, P. Basinas, G. Skodras, P. Grammelis, J.D. Pintér, S. Topis, G.P. Sakellaropoulos, A global optimization study on the devolatilization kinetics of coal, biomass, and waste fuels, Fuel Processing Technology 90 (2009) 762–769.
[36] D. Vamvuka, N. Pasadakis, E. Kastanaki, Kinetic modeling of coal/agricultural by-product blends, Energy & Fuels 17 (2003) 549–558.
[37] E. Biagini, F. Lippi, L. Petarca, L. Tognotti, Devolatilization rate of biomasses and coal–biomass blends: an experimental investigation, Fuel 81 (2002) 1041–1050.
[38] S.G. Sahu, P. Sarkar, N. Chakraborty, A.K. Adak, Thermogravimetric assessment of combustion characteristics of blends of a coal with different biomass chars, Fuel Processing Technology 91 (2010) 369–378.
[39] Y. Keheyan, PY/GC/MS Analyses of Historical Papers, Bioresources 3 (2008) 829–837.
[40] A. Sanna, S. Li, R. Linforth, K.A. Smart, J.M. Andrésen, Bio-oil and bio-char from low temperature pyrolysis of spent grains using activated alumina, Bioresource Technology 102 (2011) 10695–10703.
[41] S. Krerkkaiwan, C. Fushimi, A. Tsutsumi, P. Kuchonthara, Synergistic effect during co-pyrolysis/gasification of biomass and sub-bituminous coal, Fuel Processing Technology 115 (2013) 11–18.
[42] T. Sonobe, N. Worasuwannarak, S. Pipatmanomai, Synergies in co-pyrolysis of Thai lignite and corncob, Fuel Processing Technology 89 (2008) 1371–1378.
[43] E. Kastanaki, D. Vamvuka, P. Grammelis, E. Kakaras, Thermogravimetric studies of the behavior of lignite-biomass blends during devolatilization, Fuel Processing Technology 77–78 (2002) 159–166.
[44] A. Sanna, K. Ogbuneke, J.M. Andrésen, Bio-coke upgrading of pyrolysis bio-oil for co-firing, Fuel 88 (2009) 2340–2347.
[45] A. Sanna, J.M. Andrésen, Bio-oil deoxygenation by catalytic pyrolysis: new catalysts for the conversion of biomass into densified and deoxygenated bio-oil, ChemSusChem 5 (2012) 1944–1957.